Presented at the 21st European Photovoltaic Solar Energy Conference, September 4-8, 2006, Dresden

SOLDERING INDUCED DAMAGE TO THIN SI SOLAR CELLS AND DETECTION OF CRACKED CELLS IN MODULES

Andrew M. Gabor, Mike Ralli, Shaun Montminy, Luis Alegria, Chris Bordonaro, Joe Woods, Larry Felton
Evergreen Solar, Inc.
138 Bartlett St., Marlborough, MA 01752, 508-597-2317, agabor@evergreensolar.com

Max Davis, Brian Atchley, Tyler Williams
GreenMountain Engineering
500 Third St, Suite 265, San Francisco, CA 94107

ABSTRACT: The need to reduce PV manufacturing costs combined with the present shortage of polysilicon feedstock are driving a steady reduction in wafer and cell thicknesses. Processes, materials, and handling equipment must adapt to maintain acceptable mechanical yields and module reliability. The soldering of wires to the cells is one of the steps that becomes more challenging for thinner cells. Cells can break during the process or later crack in the modules due to damage incurred during the process. In order to maintain good yields and module reliability as we shift our String Ribbon wafer thickness below 200 microns, Evergreen Solar has developed tools to aid in process, equipment, and materials optimization and has developed improved methods of crack detection at the module level. In this paper we describe a cell breakage strength tester that we constructed as a quick feedback and quality control tool for improving and monitoring the soldering process. We also describe an electroluminescence crack detection system which we developed to give quick and nondestructive feedback for imaging the cracked cells in a module. Finite element modeling was used to explain why cells tend to crack more when loading the glass side of the modules as compared to the back side.
Keywords: Module Manufacturing, Reliability, Soldering

1 INTRODUCTION

The need to reduce PV manufacturing costs combined with the present shortage of polysilicon feedstock are driving a steady reduction in wafer and cell thicknesses. Processes, materials, and handling equipment must adapt to maintain acceptable mechanical yields and module reliability. The soldering of wires to the cells is one of the steps that becomes more challenging for thinner cells. Cells can break during the process or later crack in the modules due to damage incurred during the process. In order to maintain good yields and module reliability as we shift our String Ribbon wafer thickness below 200 microns, Evergreen Solar is studying the mechanisms involved in crack formation and is developing tools to aid in process and materials optimization and is developing improved methods of crack detection at the module level.

2 DAMAGE FROM SOLDERING

The industry conventionally interconnects cells in the modules by soldering flat solder-coated Cu wires (ribbons) from the front side of one cell to the back side of the adjacent cell. The soldering operation can occur sequentially whereby the front-side busbars are soldered first in a tabbing operation, and the back solderpads or busbars are soldered next in a stringing operation. The soldering can be done by hand or with automated equipment. Lately, the trend is toward soldering the front and rear contacts simultaneously in automated combined tabber-stringers. A variety of heat sources can be used such as hot air, IR lamps, soldering irons, lasers, and induction coils. The soldering materials, process and equipment, as well as the upstream cell processing and materials can all potentially influence the yields of the cells in the soldering process. The work below explores these issues.

2.1 Potential sources of damage

During the soldering operation, the cell and the wires heat up and expand and then later contract when the heat is removed Below the melting point of the solder, the differential contraction between the Cu and the Si, as shown by the CTE values in Table I, combined with thermal gradients, cause stress to build up in the system. In our model, this stress can cause the formation of microcracks in the Si and/or the propagation of existing microcracks. A possible solution to minimize the stress is to use wire with a lower CTE value than Cu. The literature [1] mentions Cu-clad Invar wire as a material with excellent fatigue properties that may work well in this case as the Cu can provide the required conductivity while the Ni-Fe Invar core can restrain the contraction of the wire.

Solder composition is also an important variable. Due to the low yield strength of solder, it may accommodate some stress depending on its composition and the degree of brittle intermetallic formation. The effect of using a Pb containing solder can be seen in that the temperature differential over which the wire contraction can cause damage is lower due to the lower melting point. However, Evergreen Solar has never used Pb containing solder in its interconnect wire and chose not to explore this possible solution due to the environmental concerns surrounding Pb. For this work we used our standard $Sn_{96.5}Ag_{3.5}$ composition with some level of Cu contamination due to the hot dipping method employed by the wire vendors. Still lower-temperature and softer alloys may be of interest, but these also may have module reliability concerns.

Table I: Material properties

Material	CTE	T Solidus (C)	Yield Strength (N/mm^2)
Cu	16.5		100-250
Si	2.6		brittle
Invar36	6		>550
Invar42	2		>550
$Sn_{96.5}Ag_{3.5}$	30	221	22.4
$Sn_{63}Pb_{37}$	25	183	27.3

2.2 Characterization methods

As will be discussed below, we found that when shifting our wafer thickness below 200 microns, we observed cracked cells in our modules after bending load tests. Since the cracks often intersected the soldered regions, we focused on improving the soldering operations. However, using crack data from the flexed modules was not an optimal tool to provide quick feedback during process and materials optimization. The conventional measurement used in the industry to examine the soldering process is a wire pull test whereby the force used to pull off the wires is measured and the failure interface examined. For this work we used a commercial unit from GP Solar (see Figure 1) which could record force vs distance across the busbar when pulling the wire up roughly vertical to the face of the cell.

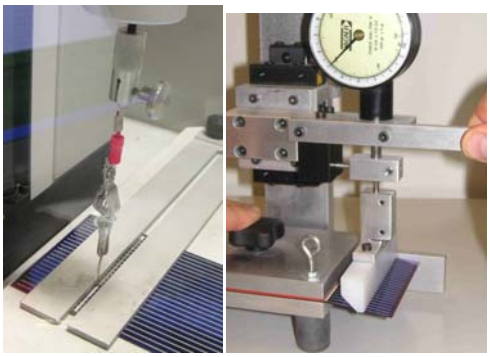

Figure 1: Wire pull strength and Cell breakage strength tests

Figure 2 shows an example of pull strength data. The peak force can be misleading since the average value can be much lower. We used the area under the curve instead. We found weak correlation between the pull strength values and the number of cracked cells found in the modules. Also, the desired interface was not obvious.

Since it was not obvious to us or others that higher pull strengths were better for either crack minimization or long term module reliability [2], and since microscopy also did not lend itself toward quick or easily quantifiable feedback, we developed a new measurement which would better correlate with the soldering damage. Figure 1 shows a breakage strength tester which clamps the cell behind the busbar region and then applies a downward force to the region of unsupported cell. The maximum downward force achieved prior to cell breakage is recorded. In particular we concentrated on the metric of the % of weak cells from the testing where the cell broke with minimal force (gauge reading <75g). We found that this data correlated well with the mechanical yield of the process and in many cases correlated to the number of cracks seen in modules. Thus, we used it to improve our understanding of the processes and to optimize the processes and materials. Also, we found that cells were weaker when tested sunnyside-up vs sunnyside-down, and so conducted most tests in sunnyside-up orientation.

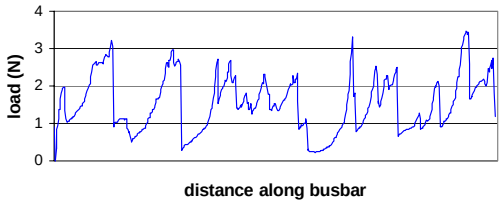

Figure 2: Wire pull strength data

2.3 Experiment and Results

In one experiment we randomized a large group of cells made from 190-micron thick String Ribbon Si wafers into 11 groups of 26 cells each. Most of the groups were then soldered under different conditions, followed by wire pull tests for 3 cells (2 wires/cell) and breakage strength tests for the remaining cells (2 tests/cell). The results are summarized in Figure 3 and discussed in the sections below.

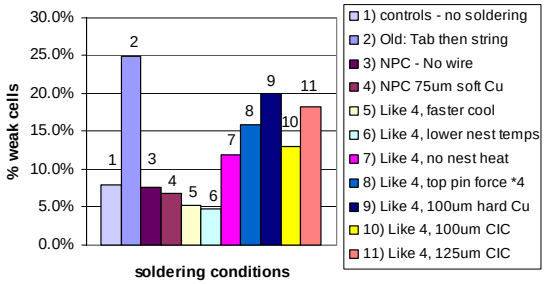

Figure 3: Cell breakage strength data

2.3.1 Machine parameters

Most of the groups were soldered using a commercial combined tabber-stringer built by NPC which uses hot air to reflow the solder and pins to press the wires against the cell on both the top and bottom side (see Figure 4). In contrast to our old sequential soldering machines whereby wires were first tabbed to the front busbar with hot air then cells were strung together on the back side in a second heating step, the NPC machine reduced the % of weak cells by a factor of 3. Indeed, the % of weak cells was not much different from the % found for the controls prior to soldering or to cells which went through the machine with no wire. Thus the machine under optimized conditions and materials did minimal damage to the cells, and some cells were found to be already weak due to upsteam processing.

One feature of the machine allows for heating the cell nests prior to, during, and after soldering in an attempt to minimize stresses due to thermal gradients, and to allow more relaxation of stress during a controlled cooldown. We found that moderate reduction of these temperatures by around 40C on average had no negative effect on soldered cell strength or wire pull strength, indicating a broad process window. Even completely turning off all nest heating had a lower effect on the % of weak cells and wire pull strength than we had anticipated, probably due the fact that machine design inherently gives some

pre and post heating from the hot air nozzles. In contrast, reducing or turning off the preheat on the old tabber machine had a more drastic effect on the soldering process window and cell breakage strength. Machines using other heat sources may also be more sensitive to the nest temperatures.

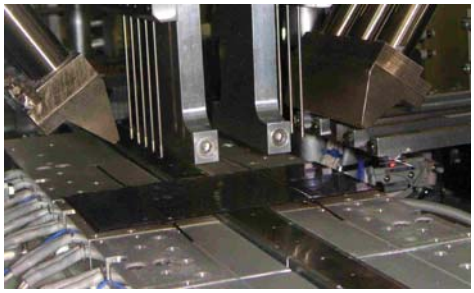

Figure 4: NPC tabber-stringer

Another machine parameter examined was the top pin force. By increasing each top pin force from roughly 30 to 120g, we found a doubling in the % of weak cells and a decrease in wire pull strength.

2.3.2 Wire parameters

We examined 4 different wires (1.54mm wide). The standard wire had 75-micron thick Cu and had been annealed to be very soft. An older generation wire with 100-micron Cu and less annealing greatly increased the % of weak cells. Cu-clad Invar-42 wire (CIC) with thicknesses (excluding solder) of 100 and 125 microns and respective Invar weight percentages of 44% and 32% were also examined. Despite the lower effective CTE of these wires and the improvements we saw with these wires in reducing cracked cells in bent modules (see section 3), these wires significantly increased the percentage of weak cells and resulted in increased mechanical yield loss during the soldering and module layup steps.

The reduction in breakage strength is consistent with the tensile load-extension curves for the wires. This data was collected on a commercial stress-strain system from Instron and is shown in Figure 5. The inflection points of the curves show the thicker wires to yield at higher loads. We conclude from the data that when soldering with the 75-micron Cu wire, damage to the silicon is minimized due to the greater compliance of the thinner and softer wire such that the Cu yields during the cooldown below the solder melting point. The lower modulus may also play a role. Harder and thicker wires are unable to yield as much and thus stress the silicon more and cause microcracks. This yielding appears to be a more important factor for the strength of the cells as measured by our breakage strength tester than the reduction in the effective CTE of the wire by the Invar. All curves were taken using wire samples directly from the spools. In practice, the wire is straightened by the soldering equipment to remove coil-set and camber, and our Instron tests showed these operations to work harden the wires a small amount. Care should be taken to cold-work the wire no more than is necessary to obtain good alignment and machine operation.

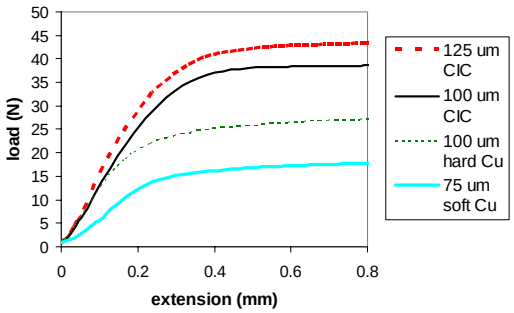

Figure 5: Instron load-extension curves for 4 different wires

The choice of wire thickness and width is part of multiparameter cost/performance optimization involving I^2R power losses, shading losses, grid design, yield losses, reliability factors, and wire cost. The relatively narrow 8-cm width of our cells allowed us to explore thinner wires than would be optimal for manufacturers with longer busbars and higher current carrying requirements.

2.3.3 Metallization effects

In addition to the soldering process, equipment, and materials variables, we found that the cell metallization process and materials also affected the soldering results. The choice of Ag paste appears to have a strong impact on the wire pull test results. Figure 6 shows an optical microscope image of a typical wire-pull failure interface for cells from condition #4 in the above experiment using Ag paste A. The failure occurs cohesively within the fired Ag busbar metallization. When using a different commercial front Ag paste (paste B), perhaps with more aggressive glass frit or different Ag particle sizes, the failure interface is typically within the Si, likely indicating some damage to the Si matrix that existed prior to soldering. In this latter case, the breakage strengths and wire pull strengths are also significantly lower. Thus, in order to optimize yields and reliability, it may be important to optimize the metallization process not only for cell efficiency, but also for mechanical strength and yield.

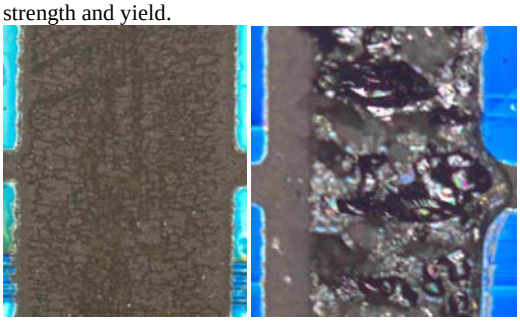

Figure 6: Wire-pull failure interfaces for paste A (left) and paste B (right).

A cell soldered using paste B was epoxy-potted, sawn along the length of the wire, then polished for cross-section SEM analysis. The image in Figure 7 shows a crack roughly parallel to the top face of the cell. This crack face is consistent with the wire pull failure interface seen where the wire easily pulls up chunks of Si. Vertical cracks are also seen in polished cross-

sections such as the one in the optical microscopy image in Figure 8. However, using cross section microscopy to hunt for and count cracks is time consuming and offers poor statistics.

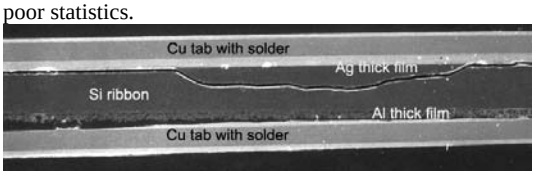

Figure 7: SEM cross section image showing a crack parallel to the cell face

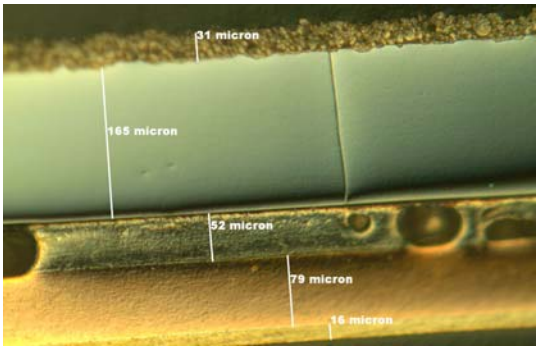

Figure 8: Optical cross section image showing a vertical crack through the Si extending along the length of the front wire

3 CRACKED CELLS IN MODULES

3.1 Crack detection

Other researchers have described how bending the modules can cause extended cracks in the cells [3]. We found this also to be the case when executing the bending load test as prescribed by IEC standard 61215 Ed.2 section 10.16. As bricks were being laid on the modules to bend them, the characteristic "pinging" sound could be heard of cells cracking. In order to detect cracked cells within modules, we developed 2 techniques.

The first technique involves shining a bright light through the backside of the module while applying about 25-30 lbs of force by hand to the glass side of the module at each cell location to separate any closed cracks. If the test is executed prior to a load test, then the applied pressure of the measurement will sometimes create cracks accompanied by the pinging sound. But if a load test is performed first, the measurement creates no new cracks. The measurement gives good information, but is laborious, gives no easily obtained image of the cracks, and causes some cracks itself. It also does not work with dark backskin.

The second technique was inspired by the photographic surveying technique described by Fuyuki [4], but uses different equipment and focuses on crack detection instead of diffusion lengths. Recent work by Trupke [5] and Takahashi [6] describes this Electroluminescence (EL) technique in more detail for mapping cell quality. Our Electroluminescence Crack Detection (ELCD) system, shown in Figure 9, comprises a digital monochrome camera (Photometrics Cascade 512b) equipped with a filter to block out visible light. We found that by forward biasing the modules in a dark room at a current about 1 to 1.5 times that of the I_{sc} rating of the module, the cells emit enough light with wavelengths < 1140nm to give a clear image with the camera and the time averaging software. In the ELCD technique, if a crack partially or fully separates a region of the cell from the wires, then this region appears darker. If a crack separates the cell into two unequal regions that each contact a wire, then the larger region appears darker than the smaller region. In general cracks are visible as dark lines, but care must be taken in interpreting images of multicrystalline material since grain boundaries, low lifetime regions, and printing defects also correspond to darker regions. Although we have largely applied the technique to modules, it also works at the unencapsulated string or cell level for crack detection.

Figure 9: Electroluminescence Crack Detection (ELCD)

Figure 10 shows ELCD images of a typical cracked cell in a module. The image on the left shows the cell with no pressure applied to the module, and the crack line can be seen below the bottom busbar. By pressing hard on the module to flex it, the crack is opened up, interrupting the continuity of current flow across the metallization pattern. This electrically isolated bottom portion of the cell is thus largely seen as dark in the middle image. After removing pressure from the module surface, the crack closes again, and apparently continuity of the metallization pattern is retained across the crack as can be seen in the rightmost image. Other dark rectangular regions in the images correspond to regions where the front Ag grid had printing defects (not visible by eye) that interrupted continuity. Other cell imaging methods that operate at short circuit conditions cannot detect such problems.

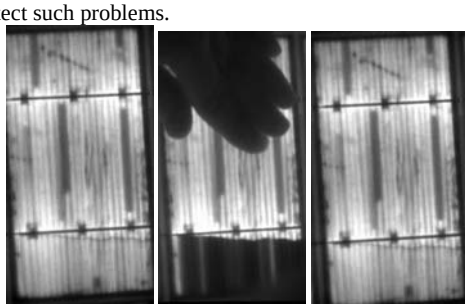

Figure 10: ELCD images before, during, and after pressing on a module above a cracked String Ribbon cell

By changing the camera lens and increasing the camera to module distance, more of the module can be imaged as is shown in Figure 11 for a load tested module with 3 cracked cells. The system could also be used to examine potential soldering-realated reliability problems where wires and underlying metallization are somehow torn from the Si surface. Figure 11 shows an

unencapsulated cell where the wires were manually pulled off from 5 of the 6 rear solder pads, leaving a signature of a brighter region around the last remaining pad. Also shown is a cell where one of the front wires was pulled up for 1 cm, leave a signature of a dark region where the front grid is isolated, and a gradient in the brightness away from the remaining busbar. Finally the system can also be used to inspect the quality of the cell binning [7]. Certain cells within a string sometimes appear overall darker or brighter than the surrounding cells. This may indicate electrical mismatch in the cell current-voltage characteristics such that at the applied current, different cells are operating at significantly different voltages.

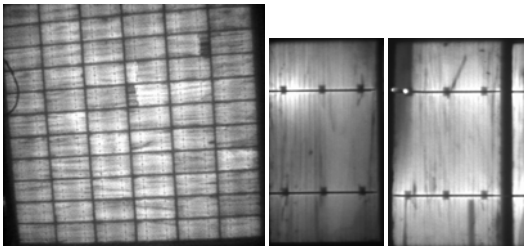

Figure 11: ELCD images of (left) part of a load-tested module with 3 cracked cells, (middle) a cell with only 1 connected rear solder pad, and (right) of a cell with the wire pulled off 1 cm of the top left busbar region

Modules from 4 different large PV manufacturers were also analyzed by ELCD both before and after load testing. A significant percentage of cells were found to contain cracks after the load testing in all cases, both for single and multi-crystalline cells. In all cases, the power degradation after load testing was below 2% or within the uncertainty of the flash IV test system. Although some cracked regions appear slightly darker, such as in the rather interesting region of the single-crystal cell in Figure 12, the great majority of cracked cells appear to have fully active area, indicating the robustness of the design. It is unclear, however, whether thermal cycling and other field exposure over many years would cause opening of tightly closed cracks and thus cause further unacceptable power degradation. Such concerns have been discussed recently by Wohlgemuth at BP Solar [8].

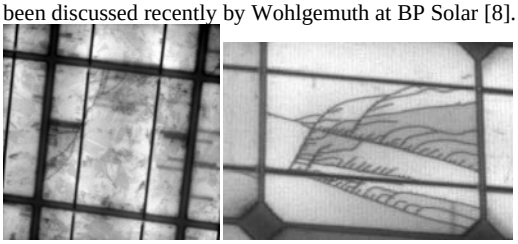

Figure 12: ELCD images of cracked multicrystalline and single crystalline cells

3.2 Module reliability

To address these module reliability issues we performed environmental chamber tests. We made six 108-cell modules with 2 of the interconnect wires described above in section 2: the standard 75 micron soft Cu wire and the 100 micron Cu/Invar/Cu wire (CIC). We applied loads with bricks sufficient to crack several cells in the Cu wire modules. The same load cracked very few cells in the modules with CIC wire. However, as is as is shown in Figure 13, even after chamber exposure well beyond the IEC-dictated 200 thermal cycles and 1000 hours damp heat, the power degradation is minimal for both cases and no convincing advantage is seen for the CIC-wire modules.

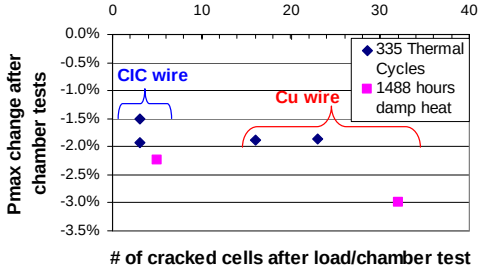

Figure 13: Module power degradation from environmental chamber testing

3.3 Crack formation and modeling

To better understand the crack formation process in the module, we built a system to perform controlled deflection of unframed laminates by applying line pressure in the center as is shown in Figure 14.

Figure 14: Laminate flex tester

During process tests, we observed cracking of cells concentrated in certain locations in the laminates (the center strings), and under certain loading conditions (when a certain threshold load was applied to the front glass, but not when the same load was applied to the rear surface of the module).

We performed analytical modeling and Finite Element Analysis to help understand the root causes of these observations. The model structure is shown in Figure 15. In particular, the analysis allowed us to:

- Map stress through the thickness and along the length of the laminate.
- Monitor where in the laminate the cells are in compression or tension.
- Understand what external conditions (loading, temperature changes) cause the stress in the cells to change from compression to tension.
- See how each of these stresses depend on system parameters such as backsheet material, EVA thickness, cell position, cell spacing, and external load.
- Understand other experimental results from the development lab and manufacturing line.

A significant finding of this analysis (see Figure 16) was that the cells are in compression after cooling from

the lamination step, but that applying a load to the glass side of the laminate can put the cells into tension (where the cells in the center strings of the module go into tension first). Certain pre-existing micro-cracks in the cells due to damage from soldering or cell fabrication processes will have a tendency to open up further and propagate into full length cracks under this tensile stress state. Conversely, applying pressure to the backskin side of the module puts the cells into a higher compressive state, thus pushing microcracks closed tighter, and this explains the lack of cracking seen by loading the back side.

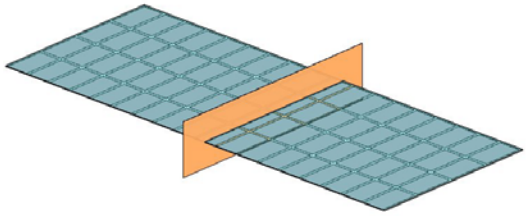

Figure 15: FEA model of the laminate

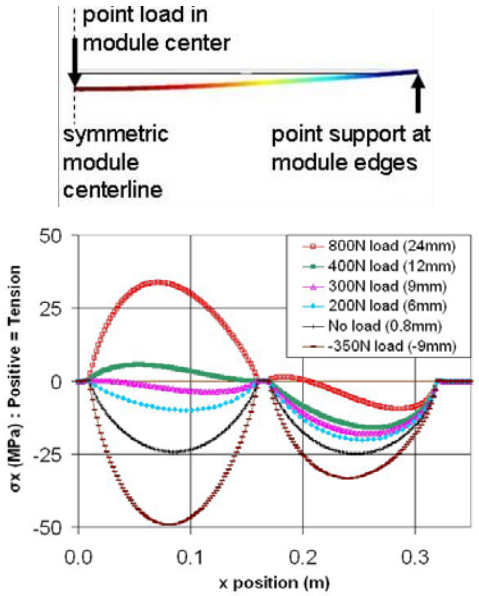

Figure 16: FEA results across the length of 2 cells in the middle and outer strings of bent laminates

The analysis further allowed us to understand how the thickness, stiffness, and other material properties of each of the module layers interacted to both change the magnitude of the stress, and to determine whether the silicon cells ever go into tension (the primary failure mode of a brittle material). This suggested how to modify these module parameters to improve yield and reliability.

4 CONCLUSIONS

Our model for the cracking of encapsulated cells involves the formation of microcracks during the metallization and soldering processes followed by tensile stresses in the bent module causing the microcracks to propagate. Softer and thinner wires aid in reducing the damage through yielding of the wire while it cools below the solder melting point. Composite wires using low expansion alloys have also been shown to reduce the tendency of cells to crack in the bent modules, but these harder and thicker wires also had the deleterious effect of reducing the strength of the as-soldered cells. More work is needed to better understand these seemingly contradictory effects.

Future questions to answer:

- Is it better to spot solder so that the damage is limited to a smaller area, or is it better to distribute the stresses more evenly over a larger area?
- How soft can the wire be made before fatigue issues arise due to the large grain sizes?
- How do the thermal stresses evolve as a function of time while cooling down from soldering?
- What do the stress field maps look like across the cell area after soldering?
- How are the stresses and damage different for wide and thin wire vs narrow and thick wire?

We intended to further extend our use of finite element analysis to help us answer some of these questions.

While we have primarily focused so far on reducing the soldering induced damage, other solutions exist to reducing cracks in modules such as stiffening and strengthening the module in its mounting configuration, and substituting solder with conductive adhesives [9].

5 REFERENCES

[1] G. R. Mon, R. G. Ross, Jr, Proc. IEEE PVSC, 1982, p. 1268.

[2] King, D. L., M. A. Quintana, J. A. Kratochvil, D. E. Ellibee, and B. R. Hansen. (2000), Progress in Photovoltaics: Research and Applications 8(2), p. 241.

[3] P. Grunow, P. Clemens, V. Hoffmann, B. Litzenburger, L. Podlowski, Proc. 20th EU PVSEC, Barcelona, Spain, 2005, p. 2380.

[4] T. Fuyuki, H. Kondo, Y. Kaji, Y. Takahashi, T. Yamazaki, and Y.Uraoka, Proc. 20th EU PVSEC, Barcelona, Spain, 2005, p. 667.

[5] T. Trupke, R.A. Bardos, M.D. Abbott, F.W. Chen, J.E. Cotter, and A. Lorenz, Proc. WCPEC-4, Waikoloa, USA, May (2006).

[6] Y. Takahashi, Y. Kaji, A. Ogane, Y.Uraoka, and T. Fuyuki, Proc. WCPEC-4, Waikoloa, USA, May (2006).

[7] H. Field and A. M. Gabor, Proc. 19th PVSEC, Paris, France, 2004, p. 2403.

[8] J. Wohlgemuth, D. Cunningham, P. Monus, J. Miller, and A. Nguyen, Proc. WCPEC-4, Waikoloa, USA, May, 2006.

[9] L. Frisson, K. Lieten, S. Reoberts, T. Bruton, Proc. 17th EU PVSEC, Munich, Germany 2001, p. 414.